Creep characteristics of clay in one-dimensional compression with unloading/reloading cycles

Propriétés de fluage des argiles en compression unidimensionnelle avec cycles de charge/décharge.

Kawabe S., Tatsuoka F.
Tokyo University of Science, Japan

ABSTRACT: One-dimensional compression tests including sustained loading stages were performed on reconstituted specimens of two types of clay. In some tests, a number of sustained loading tests were performed during otherwise multiple unloading/reloading cycles with relatively large stress amplitudes. The creep strain taking place at respective sustained loading stages is a function of the ratio of the current sustained loading stress to the stress at which the latest reversal of loading direction was made, independent of previous loading history and current sustained loading stress. A new laboratory one-dimensional compression test method is proposed to evaluate the creep process at such very low strain rates as observed in the field. Creep processes until the creep strain rate becomes as small as about 10^{-10} %/sec can be observed by this method. This new method is much less time-consuming than sustained loading tests starting from the primary loading.

RÉSUMÉ : Des essais oedométriques avec fluages ont été réalisés sur deux types d'argiles remaniées. Pour certains essais, des fluages ont ete appliqués lors de grands cycles de chargement comprenant de multiples charges/décharges. Les déformations de fluage observées sont fonction uniquement du rapport entre l' état de contrainte actuel appliqué et l' état de contrainte appliqué lors de la dernière inversion de chargement. Elles restent ainsi indépendantes de l'histoire précédant la dernière inversion et de la seule valeur de la contrainte actuelle. Une nouvelle procédure expérimentale est ainsi proposée pour étudier de manière plus précise les déformations de fluage, jusqu'à des valeurs extrêmement faibles (10^{-10} %/sec) telles que mesurées in situ. La procédure proposée a l'avantage d'écourter grandement la durée du chargement comparativement à des essais classiques de fluage réalisés lors d'une première charge.

KEYWORDS: Clay, One-dimensional compression test, Creep, Strain rate, Loading/unloading/reloading.

1 INTRODUCTION

Most of the previous studies on long-term residual compression of soft clay were focused on the behaviour during primary loading under the normally consolidated conditions. Despite strong geotechnical engineering needs, the study under general loading conditions, not only primary loading but also unloading (UL), reloading (RL) and cyclic loading (UL/RL), is very limited (e.g., Acosta Martínez et al. 2005; Kawabe et al., 2009). Besides, the concerned elapsed time under constant load after the end of construction in a full-scale soft clay deposit is usually very long. Therefore, the residual strain rates are very low, significantly lower than those in ordinary laboratory tests (Figure 1). Consequently, the field residual deformation can be predicted from ordinary laboratory test results only when based on a relevant theoretical framework that can simulate the creep behaviour at very low strain rates as in the field. However, laboratory tests to validate such a frameworks as above take extremely long time when sustained loading is performed until the strain rate reaches typical values in the field or when constant-rate-of-strain (CRS) tests are performed at typical strain rates in the field (Tanaka, 2005).

In view of the above, Kawabe et al. (2011) performed a series of one-dimensional (1D) compression tests including multiple unloading/reloading (UL/RL) cycles with many sustained loading (SL) stages on disc-shaped specimen (φ 60 mm × h 20 mm, Figure 2) made by trimming a large clay cake. The inside face of the ring was smeared with a grease layer to decrease the friction. Although the apparatus was relatively simple, CRS tests could be conducted by means of a feed-back and automated pneumatic loading system. Figure 3 summarises the relationships between the creep strain during sustained loading (SL) for three hours and the ratio of the stress at the start of unloading (UL) or reloading (RL) at an axial strain rate equal to ± 0.005 %/min, σ_{UL} or σ_{RL}, to the stress at SL, σ_{SL}. The creep strain rates during otherwise UR and RL are smaller than those during otherwise primary loading and become very small or even negative depending on loading history. Besides, positive and negative creep strains are a unique function of, respectively, the loading stress ratio, σ_{UL}/σ_{SL} (i.e., over-consolidation ratio, *OCR*) and σ_{RL}/σ_{SL}, not by the stress difference, $\sigma_{UL}-\sigma_{SL}$ and $\sigma_{RL}-\sigma_{SL}$. This relation is also a function of other factors. For example, the creep strain increases with an increase in the initial strain rate (i.e., the strain rate during the CRS loading immediately before the concerned SL stage) and the elapsed time during the SL stage.

In this study, to confirm the generality of the empirical relations described in Figure 1, another series of 1D compression tests including multiple UL/RL cycles with many SL stages were performed. Based on the test results, a new test method to observe creep behaviours at very low strain rates in a relatively short time is proposed.

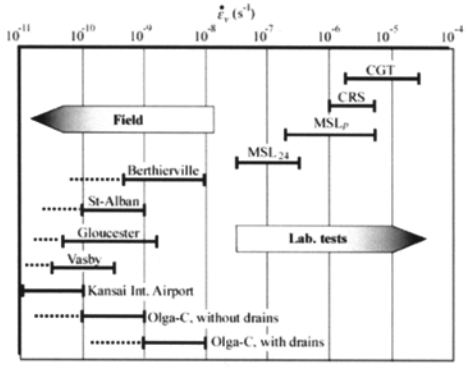

Figure 1. The strain rate measured in laboratory and in situ (Leroueil 2006)

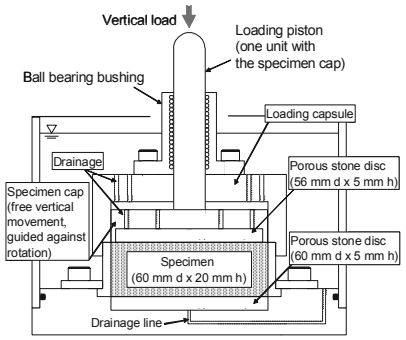

Figure 2. Oedometer used in the present study (Kongkitkul et al. 2011)

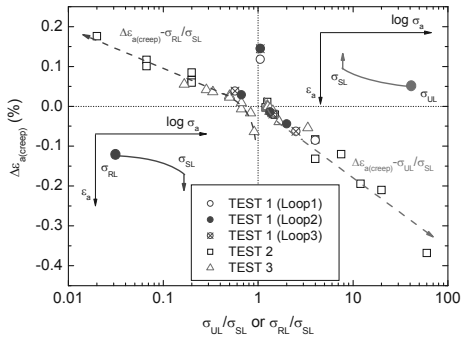

Figure 3. Relationship between the creep strain and loading stress level (Kawabe et al. 2011)

2 ONE-DIMENSIONAL COMPRESSION TESTS

The test method is basically the same as Kawabe et al. (2011). Large clay cakes of two types of reconstituted soft clay, Fujinomori clay ($w_L \approx 42$ % and PI ≈ 15) and kaolin clay ($w_L \approx 44$ % and PI ≈ 16), were produced by consolidating slurry prepared at a water content twice of the liquid limit at σ= 100 kPa in a 20 cm diameter cylinder for a week. After having applied a pre-load scheme to minimize effects of disturbance during specimen preparation, each specimen, drained at the top and bottom, was subjected to: monotonic recompression at $\dot{\varepsilon}_a$ = 0.05 %/min to σ_a = 100 kPa; SL for one day; UL at $\dot{\varepsilon}_a$ = -0.05 %/min to σ_a = 100 kPa; and SL for one day. Logarithmic axial strains are used throughout this paper. It was ensured that the specimen under the conditions described above is always essentially drained from the fact that the excess pore water pressure measured at the undrained bottom of the specimen with the drained top set in another apparatus was always less than 1 % of transient applied total axial stress (Kawabe et al. 2011). So, the measured total axial stress, σ_a , is regarded as the effective axial stress.

3 TEST RESULTS

3.1 Creep during multiple unloading/reloading cycles

In the test described in Figure 4a (test FJM1008), a number of SL stages for three hours were applied during multiple CSR UL/RL cycles changing the stress amplitude. Figures 4b and c show the time histories of σ_a and creep axial strain at each SL stage, $\Delta\varepsilon_{a(creep)}$. In Figure 4c, the data sets for the same value of σ_{UL}/σ_{SL} or σ_{RL}/σ_{SL} are denoted by the same symbol. The creep characteristics at similar value of σ_{UL}/σ_{SL} or σ_{RL}/σ_{SL} are similar, independent of loading history and axial stress at SL stage. The similar test result is shown in Figure 5. It is to be noted that these relations change with changes in the elapsed time of SL.

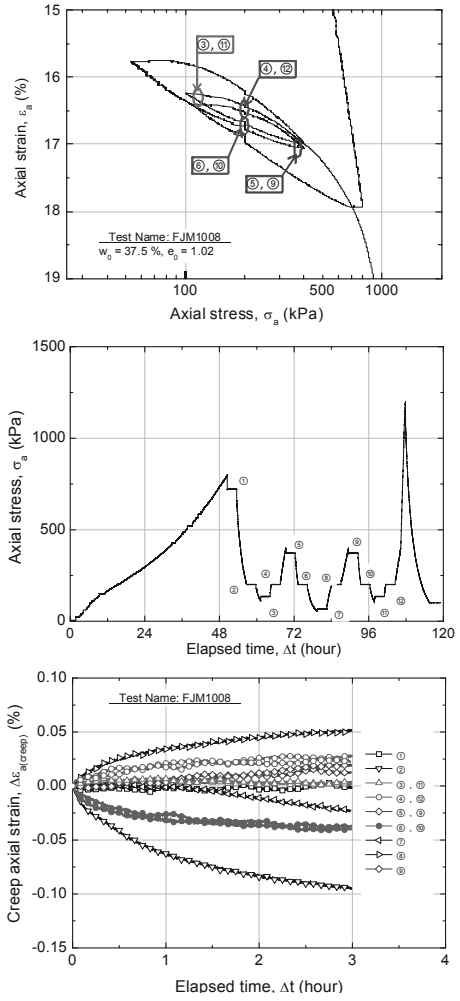

Figure 4. a) Zoom-upped $\varepsilon_a - \log\sigma_a$ relations; b) stress history; and c) time history of creep strain, test FJM1008

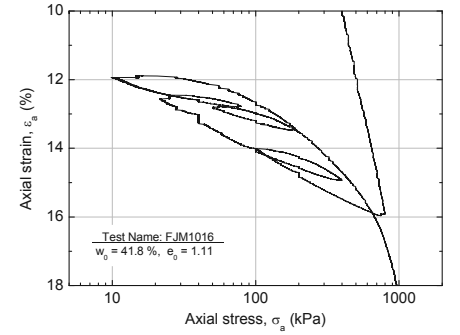

Figure 5. Zoom-upped $\varepsilon_a - \log\sigma_a$ relation. test FJM1016

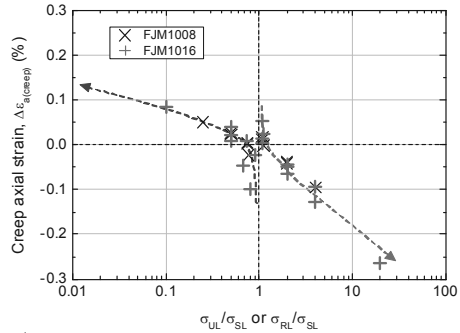

Figure 6. $\Delta\varepsilon_{a(creep)}$ - σ_{UL}/σ_{SL} or σ_{RL}/σ_{SL} relations, tests FJM1008 and FJM 1016

Figure 6 shows the relationship between $\Delta\varepsilon_{a(creep)}$ for three hours and the stress ratio, σ_{UL}/σ_{SL} or σ_{RL}/σ_{SL} , at each SL

stage, plotted in the same way as Figure 3. Also in this case, the relation is independent of loading history and stress at SL stage, and the relations for the two tests are nearly the same. This result indicates that the empirical rule presented in Figure 3 is also valid for a wide variety of loading history, at least when the void ratio range is as small as in these tests.

The current creep strain rate is controlled by the instantaneous yield characteristics. As typically seen from Figures 4a and 5, the stress at which large-scale yielding starts is not a fixed value but controlled by loading history. Kawabe et al. (2011) showed that the hysteretic stress-irreversible strain relations during cyclic one-dimensional compression of clay can be adequately described by revising the proportional rule that was originally proposed for shear tests (Tatsuoka et al. 2003). This feature is referred to below when inferring very low creep strain rates during otherwise cyclic loading.

3.2 Very low creep strain rates

Many clay types exhibit the Isotach viscous properties in one-dimensional compression (e.g., Imai 1995; Niemunis and Krieg 1996; Leroueil et al.1996; Leroueil and Marques 1996: Kawabe et al. 2011). In that case, at the '*loading*' state in the sense that the irreversible axial strain rate, $\dot{\varepsilon}_a^{ir}$, has been kept positive since the start of loading, a unique effective stress is defined for given irreversible strain and its rate. Then, the $\varepsilon_a - \log\sigma_a$ curve of a CRS test at a lower $\dot{\varepsilon}_a^{ir}$ value is located more left or lower in the plot presented in Figure 7. The $\dot{\varepsilon}_a^{ir}$ value at the strain-stress state, $(\varepsilon_a, \sigma_a)$, that is ultimately reached in any SL is zero. These zero-strain-rate states form the stress-strain relation called the reference relation. The reference relation is the same for different loading histories keeping the same sign of $\dot{\varepsilon}_a^{ir}$, but different for different loading histories changing the sign of $\dot{\varepsilon}_a^{ir}$. In Figure 7, the reference relation at the '*loading*' state and the one for the '*first unloading*' state, where $\dot{\varepsilon}_a^{ir}$ has become negative for the first time since the start of loading, are presented. Point B is located on the first unloading curve starting from point A (on the primary loading curve). During this unloading process, the total axial strain rate, $\dot{\varepsilon}_a$ $(= \dot{\varepsilon}_a^{e} + \dot{\varepsilon}_a^{ir})$ is negative, but $\dot{\varepsilon}_a^{ir}$ is kept positive while the elastic axial strain rate $\dot{\varepsilon}_a^{e}$ is kept negative with a negative axial stress rate. Note again that all the strain-stress states located right of, or above, the reference relation for 'loading', including points A, B and B', are at the 'loading' state.

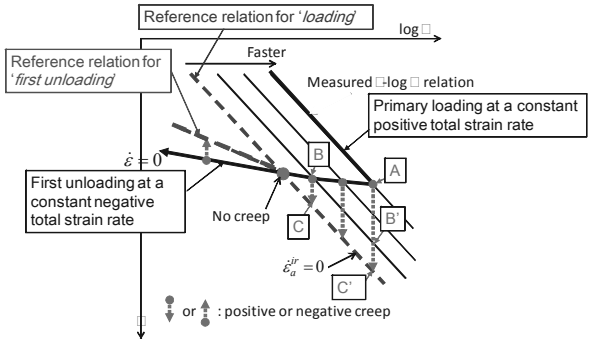

Figure 7 Illustration of $\varepsilon_a - \log\sigma_a$ and creep in Isotach theory

In SL at the '*loading*' state (where $\dot{\varepsilon}_a^{ir} > 0$), as the initial strain rate at the start of SL becomes lower, the reference relation is reached faster while the residual creep strain rate after the same elapsed time since the start of SL becomes smaller. For example, the reference relation is reached much faster when SL starts from point B than when SL starts from point A. By taking advantage of this feature, in a relatively short period by starting after having made some unloading (such as point A to point B), we can reach the creep behaviour at very low strain rates that can be observed only after a very long period when SL starts during otherwise primary loading.

Figure 8a shows the $\varepsilon_a - \log\sigma_a$ relation from a CRS test on kaolin clay, in which CRS primary loading was followed by: 1) a SL stage, SL1; 2) a small unloading; 3) another SL stage, SL2; and 4) a global RL another SL stage, SL4. Figure 8b is the zoom-up of the behaviours around the stages 1) – 3). Despite that the viscous properties of Fujinomori clay is slightly non-Isotach (Kawabe et al. 2009), the result from a similar test performed as the above (test FJM1104, cf. Figure 10) was analysed below in the framework of Isotach viscous properties.

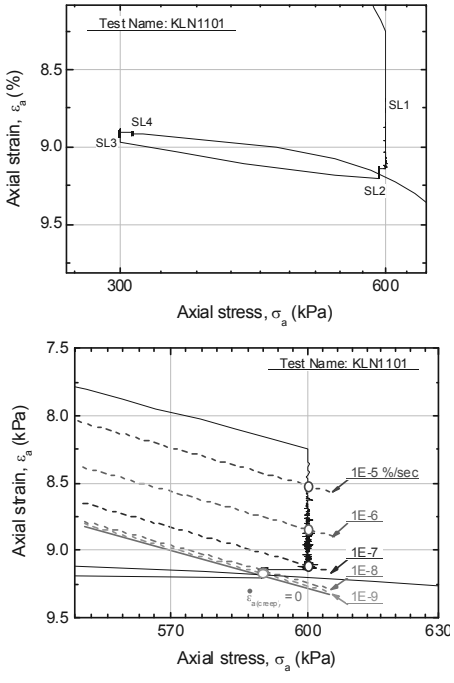

Figure 8. a) Zoom-upped $\varepsilon_a - \log\sigma_a$ relation; and b) behaviours around SL1 and SL2 stages, test KLN1101

Figures 9a and 10a show the $\log\dot{\varepsilon}_{a(creep)} - \log\Delta t$ relations from tests KLN1101 and FJM1104, where SL1 starts during otherwise the primary loading and SL2 starts during otherwise the first unloading following SL1 (see Figure 8a). It may be seen that the creep strain rate, $\Delta\varepsilon_{a(creep)}$, decreases linearly with the logarithm of the elapsed time, Δt, since the start of SL at both SL1 stages. The relations at SL1 and SL2 are different, showing that the elapsed time since the start of respective SL stages, Δt is not the parameter that controls the creep behaviours at different stresses, σ_{SL}. Figures 9b and 10b show the $\log\Delta\varepsilon_{a(creep)} - \log\dot{\varepsilon}_{a(creep)}$ relations from these two tests. The two relations at SL1 are nearly straight until $\dot{\varepsilon}_{a(creep)}$ becomes about 10^{-7} %/sec. The relations at SL2 stage are utterly different from the above.

Referring to Figure 7, according to the Isotach theory, the creep behaviour from point B to point C is equivalent to the one from point B' to point C' at the last part of the SL that has started from point A at the primary loading state. The $\dot{\varepsilon}_a^{ir}$ value is the same at points B and B' and at points C and C'. Correspondingly, in Figure 8b, the $\varepsilon_a - \log\sigma_a$ relations for different $\dot{\varepsilon}_a^{ir}$ values that are in parallel to each other have been depicted (i.e., broken lines). Each of these relations passes different $(\varepsilon_a, \sigma_a)$ states where different strain rate was observed. Following this procedure, in Figures 9b and 10b, the measured relations of SL2 have been parallel-shifted upwards to be connected to the end part of the relation of the respective SL1 stages. The combined relations can be regarded as the continuous relations that would have been obtained if SL1 had continued longer than the actual tests.

The obtained relations exhibit a drastic decrease in the slope toward eventually zero $\dot{\varepsilon}_{a(creep)}$. This trend is consistent with

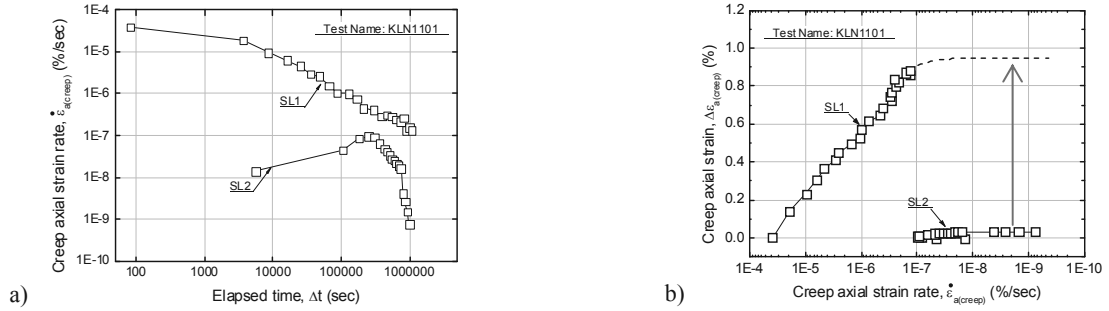

Figure 9. Test KLN1101 (SL1 and SL2): a) $\log\dot{\varepsilon}_{a(creep)} - \log\Delta t$ relations; and b) $\Delta\varepsilon_{a(creep)} - \log\dot{\varepsilon}_{a(creep)}$ relations

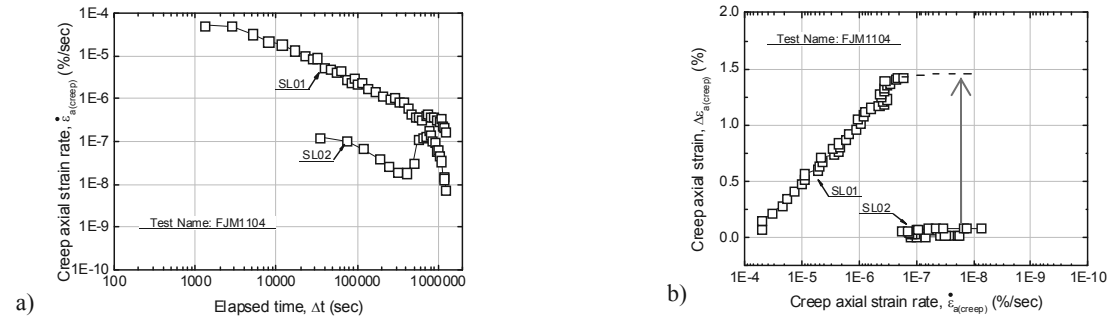

Figure 10. Test FJM1104 (SL1 and SL2): a) $\log\dot{\varepsilon}_{a(creep)} - \log\Delta t$ relations; and b) $\Delta\varepsilon_{a(creep)} - \log\dot{\varepsilon}_{a(creep)}$ relations

the Isotach theory, by which the $\dot{\varepsilon}_{a(creep)}$ value becomes ultimately zero in a given SL stage (i.e., points C and C' in Figure 7). This trend is seen in the test result presented in Figure 8b. In this figure, the reference relation, along with $\dot{\varepsilon}_{a(creep)} = 0$, has been drawn based on the value of $\sigma_{UL}/(\sigma_{SL}$ at $\Delta\varepsilon_{a(creep)} = 0) = 1.25$ that was obtained from a similar test result as those presented in Figure 3 and 6. The axial strain increment, $\Delta\varepsilon_a$, between the relations for the $\dot{\varepsilon}_a$ values different by a factor of 10 (i.e., one log. cycle of $\dot{\varepsilon}_{a(creep)}$) is similar until $\dot{\varepsilon}_{a(creep)}$ becomes about 10^{-7} %/sec, after which $\Delta\varepsilon_a$ becomes smaller towards zero as the relation approaches the reference line.

The largest advantage of the method proposed above is that creep behaviours at very low strain rates can be observed in a relatively short. This method becomes reliable when the reference relation along $\dot{\varepsilon}_{a(creep)} = 0$ is obtained from such relations as shown in Figures 3 and 6 by performing many SL during otherwise UL and RL. Extending the method described above, creep behaviours at very low strain rates (positive or negative) starting during otherwise UL/RL can be predicted by inferring the hysteresis reference relation.

4 CONCLUSIONS

The following conclusions can be derived:

1) The creep strain during normally or over-consolidated conditions after arbitrary loading history is controlled by the ratio of the stress at load reversal immediately before to the stress at sustained loading, irrespective of loading history and the stress at sustained loading.
2) With Isotach materials, creep behaviour at very low strain rates as those reached after a long period by sustained loading starting during otherwise primary loading can be observed in a relatively short period by performing sustained loading after a relevant amount of stress reversal.
3) The logarithm of creep strain rate decreases rather linearly with creep strain until the creep strain rate becomes a certain low value, followed a drastic decrease toward zero.

5 REFERENCES

Acosta-Martínez H., Tatsuoka, F., and Li, J.-Z. 2005. Viscousproperty of clay in 1-D compression: evaluation andmodelling. *Proc. 16th ICSMGE, Osaka*, 779-783.

Imai, G. 1995. Analytical examination of the foundations toformulate consolidation phenomena with inherent timedependence. *Keynote Lecture, Proc. Int. Symp. on Compressionand Consolidation of Clayey Soils, IS Hiroshima*. (2) 891-935. Rotterdam: Balkema.

Kawabe, S., Kaihara, K. and Tatsuoka, F. 2009. Non-Isotach viscous property and its simulation in drained one-dimensional compression on clay. *Proc. of 44th Conf. on Geotechnical Eng., Japan Geotechnical Society*, *Yokohama*, 237-238. (in Japanese)

Kawabe, S., Kongkitkul, W. & Tatsuoka, F. 2011. 1D Compression with Unload/Reload Cycles on Soft Clay and its Simulation. *Proc. 14th Asian Regional Conference on SMGE, Hong-Kong, CD*.

Kongkitkul, W., Kawabe, S., Tatsuoka, F. and Hirakawa, D. 2011. A simple pmeumatic loading system controlling stress and strain rates for one-dimensional compression of clay. *Soils and Foundations* 51 (1), 11-30.

Leroueil, S., and Marques, M.E.S. 1996. Importance ofstrain rate and temperature effects in geotechnical engineering. *S-O-A Report, Measuring and Modeling TimeDependent Soil Behavior, ASCE Geotech. Special Publication*. 61, 1-60.

Leroueil, S., Perret, D., and Locat J. 1996. Strain rate andstructuring effects on the compressibility of a youngclay. *Measuring and Modeling Time Dependent Soil Behavior,ASCE Geotech. Special Publication* 61, 137-150.

Leroueil, S. 2006. Suklje's Memorial Lecture – The isotache approach: Where are we fifty years after its development by Professor Suklje?. *Proc. European-Danube Conference on Geotechnical Engineering, Ljubljana,* 1, 55-88.

Niemunis, A., and Krieg, S. 1996. Viscous behaviour ofsoil under oedometric conditions. *Canadian GeotechnicalJournal* 33, 159-168.

Tanaka, H. 2005. Consolidation behaviour of natural soils around p_c value - long term consolidation test -. *Soils and Foundations*, 45(3) 83-95.

Tatsuoka,F., Masuda,T. and Siddiquee,M.S.A. 2003. Modelling the stress-strain behaviour of sand in cyclic plane strain loading. *Geotechnical and Environmental Engineering, Journal of Geotechnical and Environmental Engineering, ASCE*, 129 (6) 450-467.